High-spatial-frequency Liquid Crystal Phase Gratings with Double-sided Striped Electrodes

Lanlan Gu, Xiaonan Chen, Yongqiang Jiang, Jian Liu*, Ray T Chen

[Microelectronics Research Center, Department of Electrical and Computer Engineering, The University of Texas at Austin, Austin, TX 78758]
*[PolarOnyx, Inc., Sunnyvale, CA 94089]

Abstract

High diffraction efficiency and large diffraction angle are two major concerns in designing a liquid crystal (LC) phase grating for its applications in beam diffractive devices. High-spatial-frequency grating is capable of providing a large diffraction angle. However, fringing-field effect becomes more severe when the grating pitch size decreases, which imposes a limitation on the phase modulation depth and the diffraction efficiency of the LC grating. In this paper, a novel LC grating with striped electrodes patterned on both the top and bottom sides was proposed and fabricated. By using a specified biasing configuration, vertical electric fields are generated and well confined between the facing electrodes. Meanwhile, horizontal electrical fields are created between adjacent electrodes which help reducing the undesirable deformation of the LC director axis resulting from the fringing filed. Computer simulations show, in our novel structure, a maximum phase modulation depth of 4.15 rad (for 1.55 μm) can be achieved, which is large enough to satisfy the 1.17 π phase-shift requirement for maximum first order diffraction in sinusoidal phase gratings. Both the conventional single-sided and the novel double-sided LC gratings were fabricated and tested. Measurements showed, there was an efficiency enhancement of 77 times achieved by the double-sided structure comparing the conventional structure. A first order diffraction with diffraction angle at 14.5^o and diffraction efficiency of ~31% is experimentally achieved, of which the efficiency approaches the theoretical upper limit at 33.8% for a sinusoidal phase grating.

Keywords

liquid crystal phase grating, high spatial frequency, fringing-field effect, beam steering, binary phase grating, sinusoidal phase grating

I. Introduction

Liquid-crystal (LC) phase grating based devices have been reported for a variety of applications including projection displays, beam steering, beam slitting, beam filtering, optical switching and interconnects [1-5]. Binary LC phase gratings were extensively studied for its great capability in beam deflecting as well as its compactness and low cost fabrication [5-10]. There has been a great interest in developing a LC grating with high spatial frequency since this kind of grating is able to provide a large diffraction angle, which is a favorable feature for most beam diffractive elements.

Emerging Liquid Crystal Technologies, edited by Liang-Chy Chien,
Proceedings of SPIE Vol. 5741 (SPIE, Bellingham, WA, 2005)
0277-786X/05/$15 · doi: 10.1117/12.590095

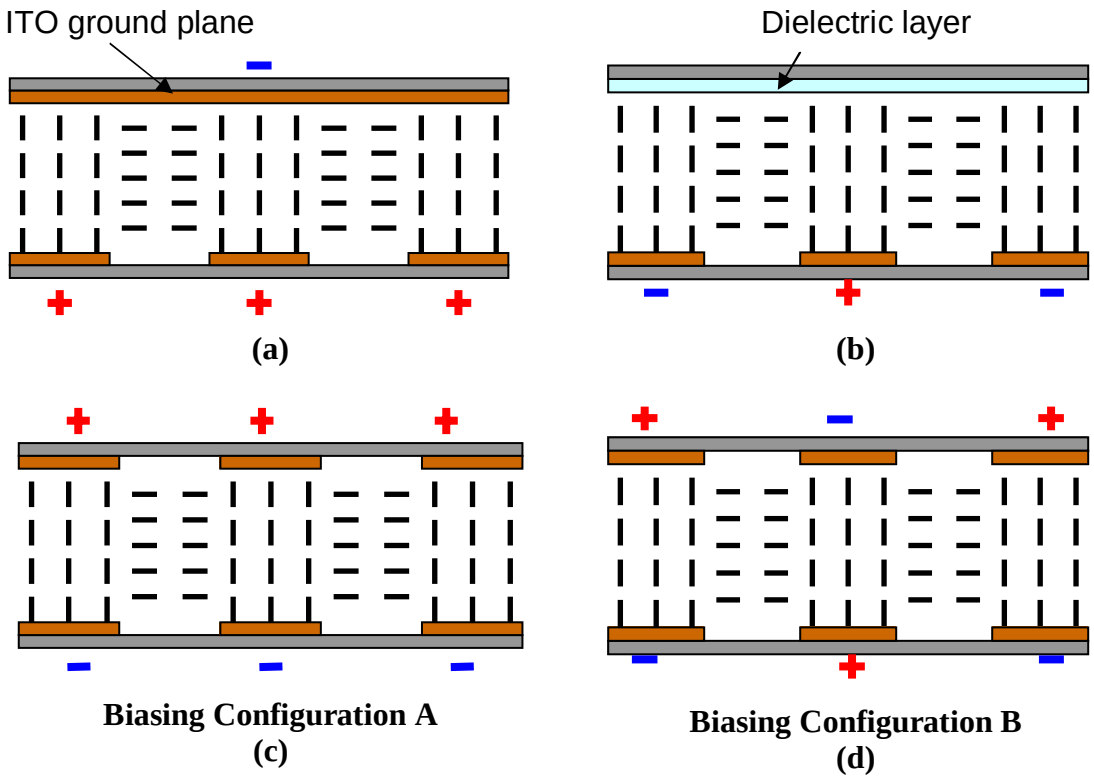

Fig. 1 Schematics of LC phase gratings:(a) Conventional single-sided structure topped with a ITO ground plane, (b) Conventional single-sided structure topped with a dielectric layer, (c) Novel double-sided structure in the biasing configuration A, (d) Novel double-sided structure in the biasing configuration B.

There are three major types of binary LC phase gratings. The simplest and most widely used one among them consists a continuous ground plane or a dielectric layer, a sandwiched nematic LC layer and a counter-plane which is periodically patterned with striped electrodes [1, 6, 7]. Two basic working mechanisms are illustrated in Fig1 (a) and (b). As shown In Fig. 1(a), homogenous (or planar) alignment is employed in a LC cell where the biasing voltage is applied between the ground plane and striped electrodes. The LC layer is initially aligned such the director axis lies either entirely perpendicular or parallel to the direction of the grating vector depending on the polarization status of the incoming beam. When the voltage is applied, vertical electric fields are generated. These fields are strong in the central regions above the striped electrodes, but weak in the lateral regions between adjacent electrodes. Ideally, the LC molecules in the central regions tend to align themselves along the field lines while those in the lateral regions are little disturbed and remain with their initial orientation. Thus, a binary spatial phase modulation is created for the incident light which is polarized in a specific direction. However, in reality, the phase modulation departs from a binary profile due to the fringing fields from the edges of the striped electrodes. These fringing fields extend into the lateral region and deform the LC director axis over there, which make the resulting phase profile more or less sinusoidal. Situation gets even worse when the spatial

frequency increases, i.e., the electrode period decreases. An overlap of the fringing fields from adjacent openings dramatically decreases the phase modulation depth, which limits the diffraction efficiency of the LC grating. Another kind of LC grating which is treated for a Homeotropic (or vertical) alignment is shown in Fig.1 (b). In this structure, the biasing voltage is applied between adjacent striped electrodes. Fringing fields are actually used to reorient the LC director along the field lines. The LC director in the central region above the striped electrode is expected to maintain its original direction, provided the electrode is relatively wide and the electric field is weak over there. But again, when the grating period and the electrode width reduce, the LC director profile is deformed in an unfavorable way. And also, the electric field in the lateral region is usually not strong enough to penetrate all the way through and whole LC layer, which largely limits the phase modulation depth of the grating. Above factors are the major reasons why they are unattractive to the application for high-spatial-frequency devices. Efforts have been made to solve the problem by developing the second and the third type of binary LC gratings [2, 8, 10]. For the second type, index matching polymer groove is used to isolate the LC regions and define the grating period. However, unlike the first type grating which can be programmed to scan the beam deflection angle, this device has only two states: on or off. It is because the pitch size of the grating is fixed since it is determined by the polymer groove. The third type of LC phase grating is constructed by using dual-alignment techniques. Basically, alignment layer is patterned and adjacent LC domains are initially aligned perpendicular to each other. When the device is off, both TE and TM waves get diffracted because both of them experience the index modulation. When the device is on, the vertical electric fields reorient the LC director uniformly along the field lines. The diffracted beams are completely extinguished since there is no existing phase modulation any more. The same problem occurs in this structure: two-state action. A more serious problem for its application in a high-spatial-frequency design is there is always an unavoidable twist deformation between adjacent LC domains. This 'twisted wall' is usually thick and limits the spatial resolution of the grating. It turns out none of these three major types of binary LC phase grating can function as a reconfigurable beam deflector with a large tuning angle and moderate diffraction efficiency. Especially, when the beam deflector works at a long wavelength such as wavelengths in the near infrared (IR) and the IR regions, the high diffraction efficiency is even harder to achieve due to the insufficient phase modulation depth, which is inversely proportional to the wavelength.

In this paper, we report a novel structure for high-spatial-frequency LC phase gratings. The large deflection angle (14.5^{o}) and the moderate diffraction efficiency (31%) was achieved simultaneously for a normally incident beam working at 1.55 μm. The schematics of our new devices are shown in fig.1(c) and (d). Homogeneous alignments are employed in our design. Compared with the conventional structures shown in fig. 1 (a) and (b), where one-sided striped electrode is used, our new device has both the top and bottom striped electrodes vertically aligned. Two specified biasing configurations are investigated. In configuration A, which is shown in Fig. 1(c), all of the striped electrodes on the top side are grounded while all of those on the bottom side are applied with the same voltage. The vertical electric fields will be generated and mainly confined between the facing electrodes. Fringing-field effect is predicted to be better suppressed. In configuration B, both top and bottom electrodes are divided into two groups. The biasing configuration follows the rule that the biasing voltage is

applied between the adjacent electrodes on the same plane and between the facing electrodes on the opposite plane as well. As seen in Fig. 1(d), this unique biasing configuration creates a horizontal electric field between adjacent electrodes and meanwhile generates a vertical electric field between facing electrodes. Horizontal fields assist in minimizing the rotation of the LC director in the lateral region while vertical fields forces the LC director in the central region orienting perpendicular to the electrode plane. An even larger phase modulation depth and together with a higher diffraction efficiency are anticipated for this promising configuration.

In this paper, director distribution of LC molecules is simulated numerically for our novel design. Phase modulation profiles are calculated and diffraction patterns are simulated by using fast- Fourier- transfer (FFT) algorithm. A brief description of the device fabrication is provided. Some of the measurement results are also presented and analyzed.

II Simulations

A simulation tool called LCD Master (Shintech Ltd., Japan) has been used by several groups to simulate the director profile under two-dimensional electric fields in LC phase gratings [1, 6, 11]. A finite-element algorithm is used in the program to calculate the director distribution through minimizing the LC free energy in the Frank-Oseen model [12]. We use a three-layer structure consisting top electrodes, LC layer, and bottom electrodes for the simulation. Input parameters of the simulated LC material E7 (Merk) include elastic constants k_{11} = 11.1pN, k_{22} = 17.1pN, k_{33} = 9pN; dielectric constants ε_s=19.0, ε_p=5.2; viscosity γ= 0.038Pas. A few assumptions are taken in the calculation: (1) strong anchoring at the substrate surfaces; (2) pre-tilt angle at 3^o, twist angle at 0^o; (3) periodic boundary.

Phase modulation profiles for a normally incident TE wave (p-wave) under different biasing conditions are obtained by using the simulated unit vector ($\hat{a}(z)$) distribution of the LC director. The x component and y component of $\hat{a}(z)$ equals $\sin\theta(z)$ and $\cos\theta(z)$, where $\theta(z)$ is the angle between the propagation direction (z direction) and the director direction ($\hat{a}(z)$). The effective index experienced by TE wave, the phase modulation profile along the grating direction and the maximum phase modulation depth are given by

$$n_{eff}(\theta) = \frac{n_e \cdot n_o}{(n_o^{\,2}\sin^2\theta + n_e^{\,2}\cos^2\theta)^{1/2}},$$

$$\phi(x) = \frac{2\pi}{\lambda}\int_0^d n_{eff}(z)dz \quad ,$$

$$\Delta\phi = \phi(x)_{\max} - \phi(x)_{\min}.$$

A thin phase-grating analysis is performed to simulate the far field diffraction pattern by using fast- Fourier- transfer (FFT) algorithm [13].

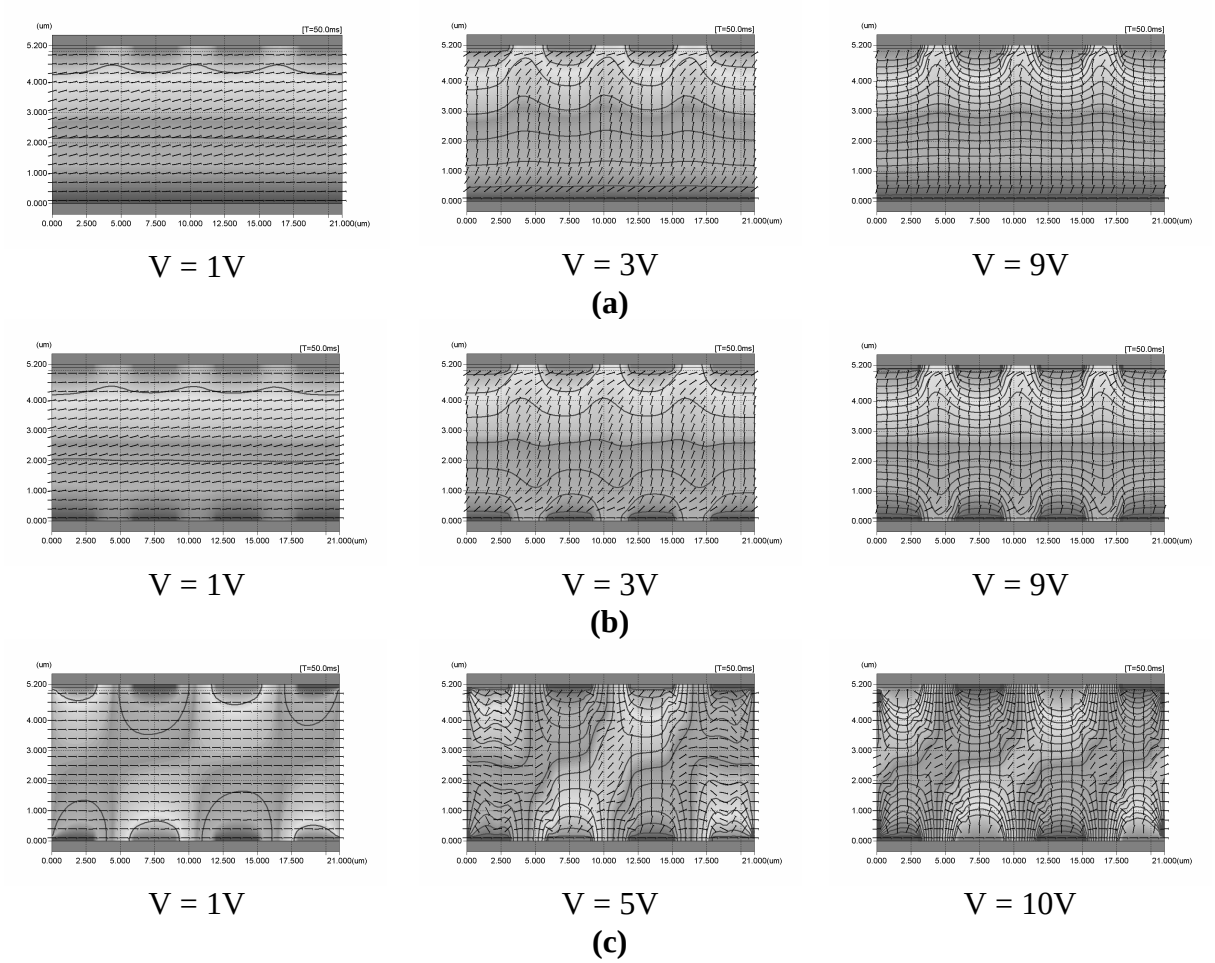

Fig. 2 LC director profiles under different biasing voltages for (a) Conventional single-sided structure, (b) Novel double-sided structure in the biasing configuration A, (c) Novel double-sided structure in the biasing configuration B.

The director profiles for the conventional single-sided structure (shown in Fig. 1(a)) and the novel double-sided structure in the biasing configuration A and B (shown in Fig. 1 (c) and (d)) are simulated. The high-spatial-frequency gratings simulated herein have the pitch size of 6 μm and electrode width of 3 μm. The thickness of the LC layer is 5 μm. For each structure, simulations are performed under various biasing voltages ranging from 1V to 10V. Some examples of the director profiles and phase modulation profiles are shown in Fig.2 and Fig.3, respectively. Fig.2 (a) shows the director profiles for a conventional single-sided structure under basing voltages at 1V, 3V and 9V. When the applied voltage is very low, the electric filed is not strong enough to switch on the LC director. With voltage increased, LC molecules in the central regions which are between the facing electrodes begin to rotate towards the direction of the electric field. However, as expected, the LC director in the lateral region is deformed undesirably by the fringing fields, which reduces the available phase modulation depth. Situation is getting even worse when the voltage increases continuously. Fringing fields become so strong that most of the directors in the lateral region are oriented vertically. Therefore, the phase modulation depth is further reduced. The improvements for the fringing-

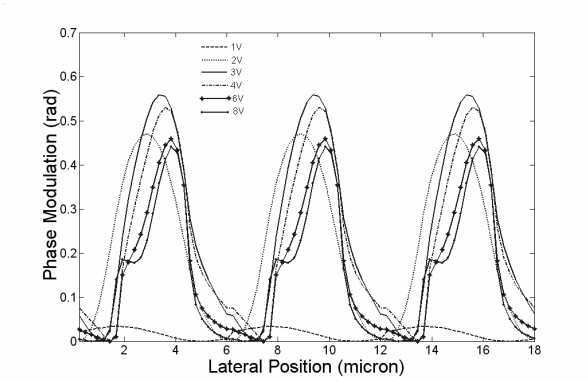

(a)

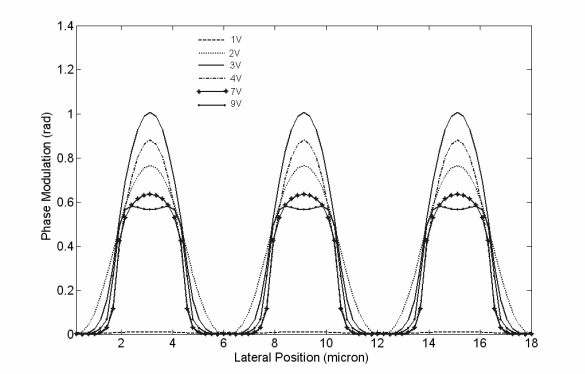

(b)

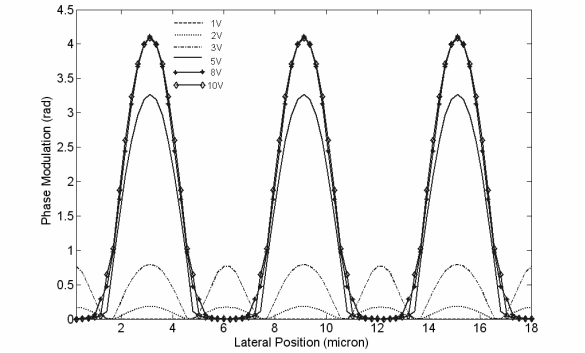

(c)

Fig. 3

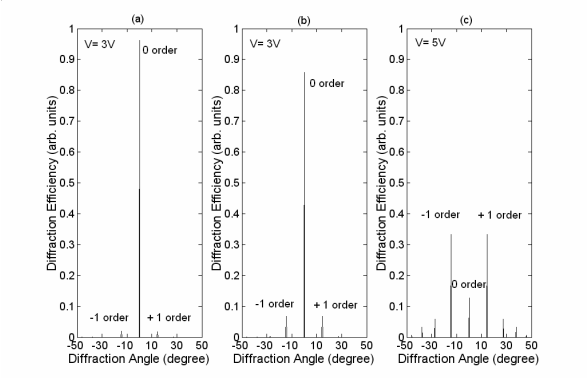

Fig. 4

Fig. 3 Phase modulations for normally incident light at 1.55μm (TE) through LC phase gratings under different biasing voltages: (a) single-sided structure, (b) double-sided structure in the biasing configuration A, (c) double-sided structure in the biasing configuration B.

Fig. 4 Far-field diffraction patterns of normally incident light at 1.55μm for the maximum first order diffraction: (a) single-sided structure, biased at 3V, (b) double-sided structure in the biasing configuration A, biased at 3V, (c) double-sided structure in the biasing configuration B, biased at 5V.

field effect in our double-sided structure are obviously shown in Fig.2 (b) and (c). Some examples of the phase modulation for both structures are shown in Fig. 3. It is evident that our double-sided structure can achieve much larger phase modulation depth than the single-sided structure. As seen in Fig. 3, the phase modulation for these high-spatial frequency gratings departs from the ideally binary profile. They are more close to sinusoidal phase gratings. The diffraction of a sinusoid phase grating is given by first-order Bessel function [13]. The theoretical upper limit for the efficiency of the first order diffraction is about 34% when the phase modulation depth reaches 1.17 π. The maximum phase modulation depths for both structures are listed in Table 1. High diffraction efficiency is expected to be achieved by using the double-sided structure in the biasing configuration B since the 1.17 π phase-shift can be

covered. Simulation shows the maximum first order diffraction efficiency for the conventional structure is only ~2%. However, by using our new double-sided structure, efficiency increases to ~6 % in the biasing configuration A and ~34 % in the biasing configuration B. Their far-field diffraction patterns are shown in Fig.4. The zero order diffraction is efficiently suppressed by the first order diffraction in our double-sided structure, which is cleared presented in Fig. 4(c).

	Theoretical predictions			Experimental results	
	Maximum phase shift (rad)	Maximum efficiency	efficiency Enhancement (times)	Maximum efficiency	efficiency Enhancement (times)
Single-side	0.54	~ 2%	1	~ 0.4%	1
Double-side A	1.01	~ 6%	3	~ 2%	5
Double-side B	4.15	~ 34%	17	~ 31%	77

Table 1

The computer simulation confirmed theoretically that our novel double-sided structure in a specified biasing configuration provides a good solution to the fringing-fields effect, which intrinsically occurs in the high-spatial-frequency reconfigurable LC phase gratings. The maximum achievable diffraction efficiency for our designed structure approaches the theoretical upper limit of a sinusoidal phase grating.

III Experiments and Discussions

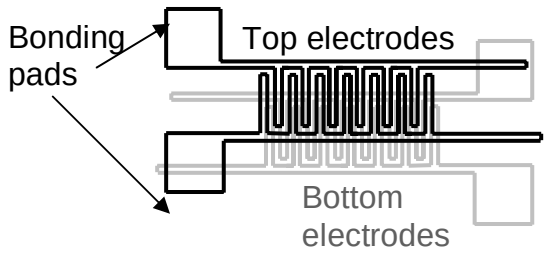

Fig. 5 The schematic of the electrode pattern and the electrode alignment.

Both single-sided and double-sided LC gratings are fabricated. The grating pitch size and electrode width of our devices are 6 μm and 3 μm, respectively. The thickness of the LC layer is 5 μm. Fig. 5 shows the designed electrode pattern and the electrode alignment schematically. Striped electrodes are pattern on the ITO coated glass by conventional photolithograph and wet etching techniques. The alignment layer of polyimide PI2556 (HD MicroSystems) was spin-coated on the glass substrate. It followed by a rubbing treatment. For the double-sided grating, the top electrodes and bottom electrodes are aligned by using the conventional mask aligner. A uniform gap between the top and the bottom substrate was formed by using glass micro-beads. A nematic LC material with a positive dielectric anisotropy E7 (Merk) was filled into the cell under room temperature. For better initial alignments, the LC cell was heated to above its clearing point after being sealed by UV glue. A 1.55 μm laser was used for the optical characterization. A linear polarizer was placed between the laser and device to control the polarization of the incident beam. An ac voltage with frequency of 150Hz was applied on the devices.

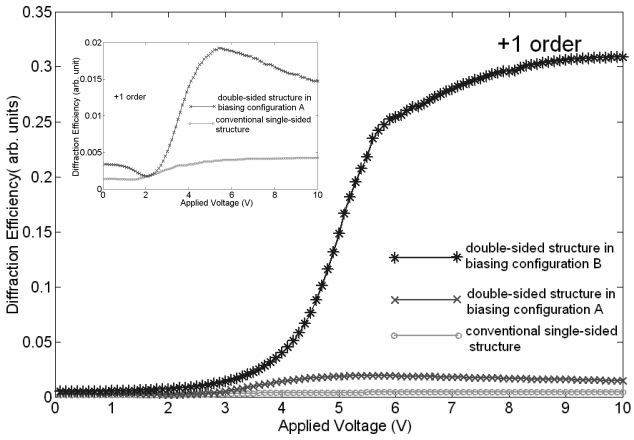

Fig. 6 Measured efficiency of the first order diffraction as a function of the applied voltage for the single-sided structure and the double-sided structure in the biasing configuration A and B.

The first order diffraction efficiencies for the single-sided structure and the double-sided structure in the biasing configuration A and B were measured, respectively. The diffraction intensity was normalized to the transmission intensity of the grating when there was no biasing voltage applied. In Fig. 6, a huge enhancement of the diffraction efficiency from our double-sided device can be easily observed. For a voltage scanning starting from 0.1V to 10V, the maximum efficiency we achieved for the double-sided device (in configuration B) was about 31% while only the efficiency of 0.4% was achieved by the conventional single-sided device. The efficiency was increased by approximately 77 times. There was an efficiency enhancement for the biasing configuration A too. Comparing with the single-sided structure, its diffraction efficiency increases by 5 times, which is clearly shown in the insert of Fig. 6. It provides the evidence the fringing-field effect can be reduced by using the stripe-to-stripe structure, even without using the elaborately designed biasing configuration. Both theoretical predictions and the experimental results are listed and compared in Table 1. The measurement of the double-sided structure in the biasing configuration B is in a good agreement with the theoretical prediction. It approaches the theoretical upper limit of a sinusoid phase grating. However, the diffraction efficiency measured from the single-sided structure and the double-sided structure in the biasing configuration A are below the simulated values. These phenomena can be explained as follows. In the simulation, we assume there is no twist deformation of the LC director. We also assume the pre-tilt angle of 3^o. However, twist deformations can not be completely avoided in our system owing to the manually controlled the rubbing process. Also, the actual pre-tilt angle of our LC director maybe smaller than the value we assumed in the simulation. Above two factors would have negative influences on the phase modulation and, consequently, degrade the performance of the LC gratings. However, it doesn't affect much in the performance of our double-sided structure in the biasing configuration B. This is because, theoretically, its phase modulation depth can reach far beyond 1.17 π (0.585λ), which is ideal to achieve the maximum first order diffraction in the model of sinusoidal phase gratings. Therefore, the targeted 1.17 π phase-shift is achievable even though it may encounter a reduction in the available phase modulation depth.

IV. Conclusions

We proposed a novel structure for high-spatial-frequency liquid crystal phase gratings. The main idea is to overcome the fringing-field effect, which is a serious problem limiting the diffraction efficiency for a high-spatial-frequency LC phase grating, by using a double-sided structure, where the striped electrodes are patterned on both the top and bottom sides. By using a specified biasing configuration, vertical electric fields are generated and well confined between the facing electrodes. Meanwhile, horizontal electrical fields are created between adjacent electrodes which help reducing the undesirable deformation of the LC director owing to the fringing-field effect. Thus, a much larger phase modulation depth can be achieved compared with the conventional single-sided structure. This idea was theoretically and experimentally confirmed. Computer simulation shows the maximum phase modulation depth can be achieved by our new structure is 4.15 rad (for 1.55 μm), which is large enough to cover the 1.17 π phase-shift which is ideal to the first order diffraction of a sinusoidal phase grating. However, the achievable phase modulation depth in the single-sided structure is only 0.54 rad. Both single-sided and double-sided devices were fabricated and tested. Measurements showed the first order diffraction was enhanced by 77 times using our doube-sided structure. The first order diffraction with diffraction angle at 14.5^{o} and diffraction efficiency of 31% was experimentally achieved. Our double-sided LC phase grating is attractive for the applications in beam deflecting and beam steering devices which work in the near IR and IR regions.

References:

[1] Ichiro Fujieda, "Liquid-crystal phase grating based on in-plane switching," Applied Optics, vol. 40, pp. 6552-6209, 2001.

[2] Hajime Sakat, and Michiyo Nishimura, "Switchable Zero-Order diffraction filters using fine-fitch phase gratings filled with liquid crystal," Jpn. J. Appl. Phys., vol. 39 , pp. 1516-1521, 2000.

[3] Boris Apter, Uzi Efron, and Eldad Bahat-Treidel, "On the fringing-field effect in liquid-crystal beam-steering devices," Applied Optics, vol. 43, pp. 11-19, 2004.

[4] D. P. Resler, D. S. Hobbs, R. C. Sharp, L. J. Friedmanks, and T. A. Dorschner "High-efficiency liquid-crystal optical phased-array beam steering," Optics Letters, vol. 21, pp. 689-691, 1996.

[5] Jae-Hong Park, Chang-Jae Yu, Jinyool Kim, Sung-Yeop Chung, and Sin-Doo Lee, "Concept of a liquid-crystal polarization beamsplitter based on binary phase gratings," Applied Physics Letter, vol. 83, pp. 1918-1920, 2003.

[6] Manuel Bouvier, and Toralf Scharf, "Analysis of nematic-liquid-crystal binary gratings with high spatial frequency," Opt. Eng., vol. 39, pp.2129-2137, 2000.

[7] R. G. Lindquist, J. H. Kulick, G. P. Nordin, J. M. Jarem, S. T. Kowel, and M. Friends "High-resolution liquid-crystal phase grating formed by fringing fields from interdigitated electrodes," Optics Letters, vol. 19, pp. 670-672, 1994.

[8] J. Chen, P. J. Bos, H. Vithana, and D. L. Johnson," An electro-optically controlled liquid crystal diffraction grating," Applied Physics Letter, vol. 67, pp. 2588-2590, 1995.

[9] Chang-Jae Yu , Jae-Hong Park, , Jinyool Kim, Min-Sik Juang, and Sin-Doo Lee, "Design of binary diffraction gratins of liquid crystals in a linearly graded phase model," Applied Optics, vol. 43, pp. 1783-1787, 2004.

[10] Mary Lou Jepsen and Hendrik J. Gerritsen, "Liquid-crystal-filled gratings with high diffraction efficiency," Optics Letters., vol. 21, pp. 1081-1083, 1996.

[11] Ichiro Fujieda, Osamu Mikami, and Atsushi Ozawa "Active optical interconnet based on liquid-crystal grating," Applied Optics, vol. 42, pp. 1520-1525, 2003.

[12] M. Kitamura, "Computer simulation of director profile in two dimensional electric fiedl ," SID-IDRC, pp350-353, presented at the International Display Research Conference, Monterey, CA, 1994.

[13] J. W. Goodman, Introduction to Fourier Optics, pp. 81-83, McGraw-Hill, New York(1996)

.